Liquid Crystals
Publication details, including instructions for authors and subscription information:
http://www.informaworld.com/smpp/title~content=t713926090

Experimental investigations of a chiral smectic glass-forming liquid crystal

I. Dierking[a]
[a] School of Physics and Astronomy, University of Manchester, Schuster Building, Manchester M13 9PL, UK

To cite this Article Dierking, I.(2008) 'Experimental investigations of a chiral smectic glass-forming liquid crystal', Liquid Crystals, 35: 8, 1015 — 1022
To link to this Article: DOI: 10.1080/02678290802309447
URL: http://dx.doi.org/10.1080/02678290802309447

Liquid Crystals,
Vol. 35, No. 8, August 2008, 1015–1022

Taylor & Francis
Taylor & Francis Group

Experimental investigations of a chiral smectic glass-forming liquid crystal

I. Dierking*

School of Physics and Astronomy, University of Manchester, Schuster Building, Oxford Road, Manchester M13 9PL, UK

(Received 3 March 2008; final form 22 June 2008)

Experimental results are reported for a chiral smectic A (SmA*) liquid crystalline cholesteryl-carbonate, which suggest an unusual transition into a glassy state for a low molar mass mesogen. The glass transition is accomplished over a time period of several days at room temperature. It involves two processes, which are attributed to freezing of the mobility of the phenyl-containing flexible tails and subsequent glass formation of the bulky cholesteryl groups of the material. During the glass formation process no texture changes are observed and the qualitative electro-optical response is retained. This subtleness of the transition is also exemplified by only minute features in respective DSC curves. Deviations from the common electroclinic temperature dependence are observed below a temperature within the SmA* phase. During a second process at lower temperature, the electro-optical switching then diminishes and a strongly increasing viscosity is observed with time.

Keywords: chiral smectic A phase; glass-forming liquid crystal; cholesteryl-carbonate

1. Introduction

More than a century ago, cholesteryl derivatives where the first liquid crystalline (LC) compounds to be discovered (*1, 2*). Due to the availability of cholesteryl as a natural product, it was widely used in the synthesis of LC compounds in the beginning of the 20th century (*3*) and a whole range of these derivatives is commercially available in large quantities (several grams) at virtually no cost. The vast majority of these compounds exhibit LC blue phases, the cholesteric (chiral nematic, N*) phase and the fluid chiral smectic A (SmA*) phase, but also the rare occurrence of the ferroelectric chiral smectic C (SmC*) phase has been reported (*4*). The high viscosity of cholesteryl derivatives has diminished interest in their direct exploitation for commercial liquid crystal applications, although their high helical twisting power offers use of these materials as chiral dopants in LC mixtures.

The transition of fluids into a glassy state (*5–7*), in contrast to crystallisation, has retained the interest of scientists for several decades and has been employed in material manufacture for several thousands of years (*8, 9*). Glasses are amorphous solids, which are formed by supercooling a liquid quickly enough to prevent molecular rearrangement into a three-dimensionally ordered structure, skipping the crystallisation's nucleation and growth process. From a structural point of view, the disorder of the high-temperature liquid phase is retained, whereas the characteristic molecular motion of the liquid is practically absent. Glasses can thus be regarded as a 'snapshot' of the high-temperature phase. In principle, all materials are potential glass formers; it is just a question of the appropriate cooling rate. For materials with a large viscosity over a wide temperature range and a slow crystallisation process, glass formation is relatively easy to obtain. For materials with a low viscosity and rapid crystallisation, very large cooling rates have to be applied. The best-known example of a glass is obviously window glass, made from sand, lime and soda since hundreds of years, but also optical fibres or amorphous silicon and germanium used in solar cell devices are commonly known amorphous solids (inorganic glasses). Most technologically employed polymers exhibit a transition into a glassy state (organic glasses) or at least an only partially crystalline state, including biopolymers such as cellulose (*10, 11*). Even metals and alloys can be forced into a non-equilibrium glassy state by cooling with rates in the order of $10^6\,\mathrm{K\,s^{-1}}$ (*12, 13*). The glass state is characterised by mechanical and viscous properties comparable to those of a solid, while retaining the structural disorder of the high temperature liquid.

This is the point where the anisotropic properties of self-organised liquid crystals as a high-temperature phase become important. Just like the disorder of an isotropic liquid is 'frozen' by forming a glass, so is the orientational (nematic) or additional positional (smectic) order, if a glass is formed from the LC state. This allows the formation of partially ordered glasses while being able to select the direction of order, i.e., for example, the optical axis, by application of electric or magnetic fields during cooling. Similarly, polar glasses may be formed, if the high

*Email: ingo.dierking@manchester.ac.uk

ISSN 0267-8292 print/ISSN 1366-5855 online

DOI: 10.1080/02678290802309447
http://www.informaworld.com

temperature LC phase is composed of chiral molecules. This can be achieved via the electroclinic effect (*14*) in a glass-forming SmA* phase or by employing glass-forming ferroelectric SmC* liquid crystals in the surface stabilised geometry (*15*). Possible applications include phase plates, optical information storage, holography (*16*) or second harmonic generation (SHG) by materials, which can variably be realigned by heating into the LC state, orientation selection by external fields and subsequent cooling into the glass state. A number of reports of low molar mass glass-forming liquid crystals can be found in the literature. These even include standard materials such as MBBA, rapidly quenched in liquid nitrogen (*17, 18*), but also materials, which exhibit nematic or smectic glasses at room temperature (*19–23*), obtained by moderate cooling rates. In some cases isotropic, nematic and smectic glasses can all be obtained by simple variation of the length of the mesogenic bridging group (*24*). The fact that cholesteryl-based liquid crystals exhibit a rather high viscosity and slow crystallisation kinetics (minutes to hours) as compared to other conventional calamitic liquid crystals makes them prime candidates for obtaining glasses from LC phases. This study reports a detailed account of a SmA* cholesteryl-carbonate with a transition into the glass state, which is accomplished via a two-step process, without changing the structure of the high-temperature phase.

2. Experimental

The investigated cholesteryl-carbonate has the structural formula shown in Scheme 1, which is very similar to compounds discussed by Vill *et al.* (*4*). Its phase sequence as determined by polarising optical microscopy, electro-optical and current investigations is obtained as: I 60°C SmA* 38°C SmA* ~RT glass (on cooling) and will be discussed in detail below.

Differential scanning calorimentric (DSC, Mettler-Toledo DSC 822E) measurements were carried out at varying heating and cooling rates in the range 5–20 K min^{-1}. Samples for electro-optical investigations were prepared by filling commercially available sandwich cells of gap $d=4\,\mu m$ (EHC, Japan) by capillary action in the isotropic phase. These were placed in a polarising optical microscope (Zeiss), equipped with a Mettler FP52 hot-stage for control of relative temperatures to 0.1 K. Electric fields were applied by a standard function generator (Leader LFG-1300), in combination with a high-voltage amplifier F400D from FLC Electronics and the electro-optical response was monitored on a Tektronix TDS 540 digital storage oscilloscope. Applied electric field amplitudes were 20 V μm^{-1} at square waveform, unless otherwise indicated.

The switching angle ϕ of the electroclinic effect was determined from the electro-optical transmission modulation according to a method outlined by Rudquist (*25*). Depending on the amplitude of the response, up to 2000 individual transmission curves were averaged to reduce statistical noise. Similarly, the response times, τ, were determined from the electro-optical modulation for applied square wave electric fields, changing from 10% to 90% transmission. Reversal current measurements were carried out by the well-known triangular wave method (*26*).

3. Experimental results and discussion

DSC traces of the compound are shown in Figure 1 for both heating and cooling cycles. Having left the material untouched for about eight years, the very first heating curve shows that over the period of years the compound has in fact crystallised, as exemplified by a first order transition centred at 53°C. A subsequently observed much smaller peak centred at about 70°C corresponds to the SmA*–isotropic transition. This behaviour is not observed for any subsequent heating runs (Figure 1(a)). On heating, a typical glass transition into the SmA* phase is observed at approximately 5°C, whereas the clearing temperature is still centred at about 70°C. The transition at low temperatures is indeed a glass

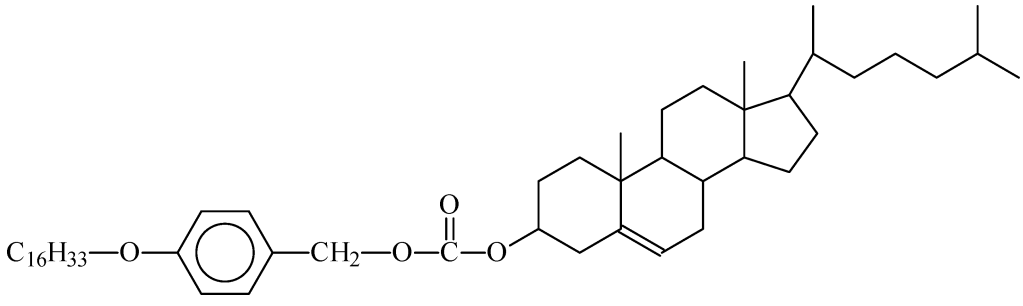

Scheme 1. Structure of the cholesteryl-carbonate investigated.

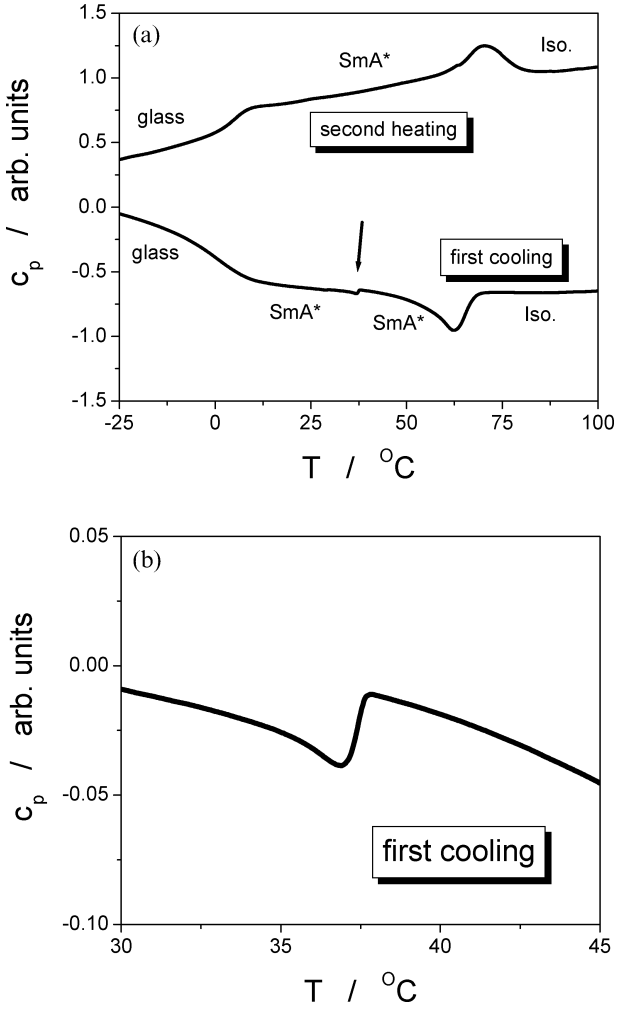

Figure 1. (a) First cooling and second heating DSC traces, which demonstrate the glass transition at approximately 5–10°C and the clearing temperature at about 60–70°C. Especially on cooling, a small feature resembling a transition within the SmA* phase is observed, indicated by an arrow. (b) Detail of the DSC cooling curve in the vicinity of the transition within the SmA* phase. The transition appears to be of almost second order, with no changes in texture or qualitative electric and electro-optical properties observed. It is anticipated that this transition may be related to a change from a non-intercalated to an intercalated structure on cooling.

transition, because on heating a step increase in the heat capacity at constant pressure, c_p, is observed. On cooling, the DSC traces suggest a transition centred at approximately 38°C and a glass transition at about 10°C (see Figure 1(a)). The rather small feature observed at 38°C displays an increase in heat capacity on cooling, which suggests that this is related to a second-order phase transition. Nevertheless, it should be noted that this does not represent a transition into the ferroelectric SmC* phase, as will be demonstrated below. In general, the DSC temperatures correspond quite well with those observed from electro-optical experiments (see below).

In sandwich cells the clearing temperature of the investigated compound is approximately $T \approx 60$°C, with a relatively broad two-phase region of about 5 K being observed. Very slow cooling across this transition results in a well oriented planar texture of the SmA* phase. As will be demonstrated in more detail below, the change in physical properties indicates a transition at $T = 38$°C, but without being accompanied by any texture changes. Based on the behaviour of the electro-optical response and the current reversal curves, we believe that the state below 38°C is still SmA*, but with a strongly hindered mobility of at least parts of the molecules. Evidence for this behaviour is depicted in Figure 2, where exemplary measurements of the transmission and the current response are shown for applied triangular electric fields for temperatures above (Figure 2(a)) and below (Figure 2(b)) the discussed transition. In both cases the transmission linearly follows the applied electric field and absolutely no indications of a current reversal peak are observed, as it would be expected for a transition into SmC*.

A completely analogous behaviour is observed for applied square-wave and sine-wave fields. Figure 3 shows the dependence of the induced tilt angle ϕ on applied electric field amplitude, E. The behaviour is linear, with increasing tilt for increasing field and clearly indicates the observation of electroclinic switching (*14*).

The temperature dependence of the induced tilt angle ϕ is depicted in Figure 4(a). It is found to strongly increase with decreasing temperature, as expected for the electroclinic effect. The dependence of the electroclinic tilt ϕ on temperature, T, and electric field amplitude, E, is generally described by the relation:

$$\phi = \frac{\chi_0 \varepsilon_0 c^*}{\alpha (T - T_C)} E, \qquad (1)$$

where χ_0 is a generalised susceptibility, ε_0 the permittivity of free space, c^* the chiral coupling coefficient, α the first Landau expansion coefficient and T_C a transition temperature into a low-temperature phase [see Lagerwall (*27*), chapter 5.8]. From Equation (1) it can readily be seen that for constant temperature, ϕ increases linearly with the electric field, as demonstrated in Figure 3. Approaching T_C from above, ϕ is expected to diverge, as depicted in Figure 4 a. The experimentally observed behaviour is thus clearly reminiscent of the electroclinic effect. Referring to Equation (1), the induced tilt should be inversely proportional to temperature. But a closer

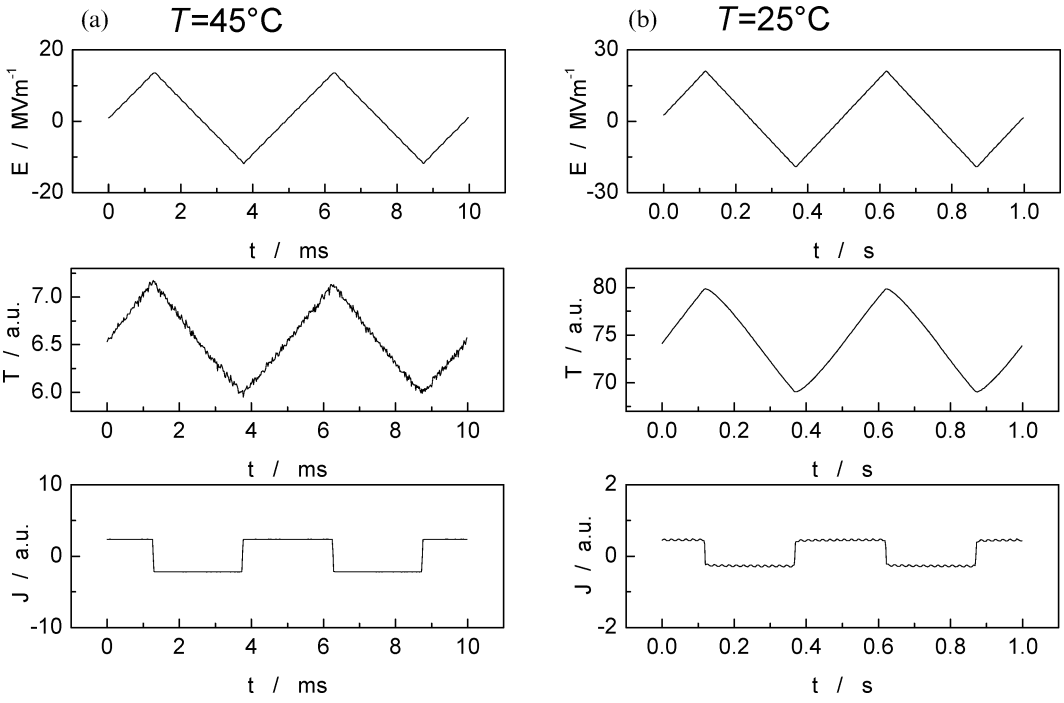

Figure 2. Applied electric field (top), electro-optical response (middle) and current response (bottom) at (a) T=45°C above the transition within SmA* and (b) T=25°C below the transition. From the measurements it is apparent that through the discussed transition at T=38°C any qualitative behaviour of the SmA* phase, such as the linear electro-optic response, is clearly retained and no indications of a current reversal peak are observed.

inspection of the experimental data depicted in Figure 4(a) shows that the temperature dependence of the induced tilt can not be described by a single reciprocal functionality. This is illustrated by the solid line, which represents the best fit according to Equation (1), covering the whole range of investigated temperatures. The discrepancy becomes more apparent when plotting the induced tilt ϕ as a function of reciprocal temperature $1/T$, as depicted in Figure 4(b). For temperatures above approximately 38°C the induced tilt follows a linear relationship in $1/T$, whereas for lower temperatures a nonlinear behaviour is observed. This indicates a change in physical properties at around T=38°C, whereas the macroscopic phase appearance and the general electro-optical behaviour is retained.

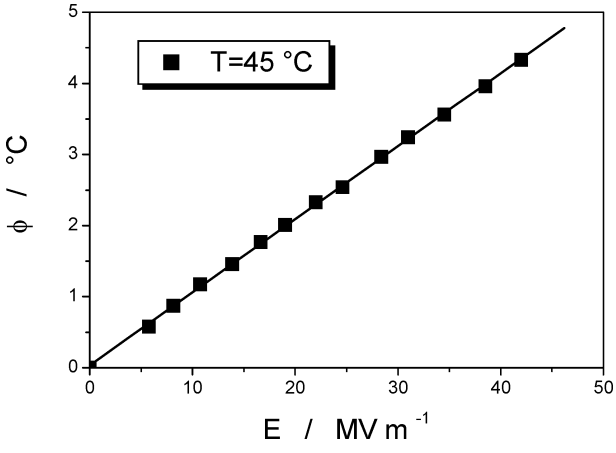

Figure 3. Demonstration of the electroclinic behaviour of the electro-optical response in the SmA* phase at 45°C. A linear increase of the induced tilt angle ϕ is observed for increasing electric field amplitude, E, as expected from Equation (1).

Figure 5 shows the response times, τ, measured on cooling from the isotropic phase (closed squares), as well as on heating after tempering the sample for 24 h at T=25°C (open triangles). During the tempering process the response time increases by a factor of five, but on subsequent heating, again at a temperature of approximately $T\approx$38°C, it resumes an identical temperature dependence to that observed on cooling. This is a further clear indication that at this temperature a transition takes place, as already indicated by the DSC measurements (Figure 1(b)).

The temperature dependence of the electroclinic response time, τ, is given by:

$$\tau = \frac{\gamma}{\alpha(T - T_C)}, \qquad (2)$$

where γ is an effective viscosity (see Lagerwall (*27*), chapter 5.9). The switching time is thus independent of electric field amplitude and diverges on approaching

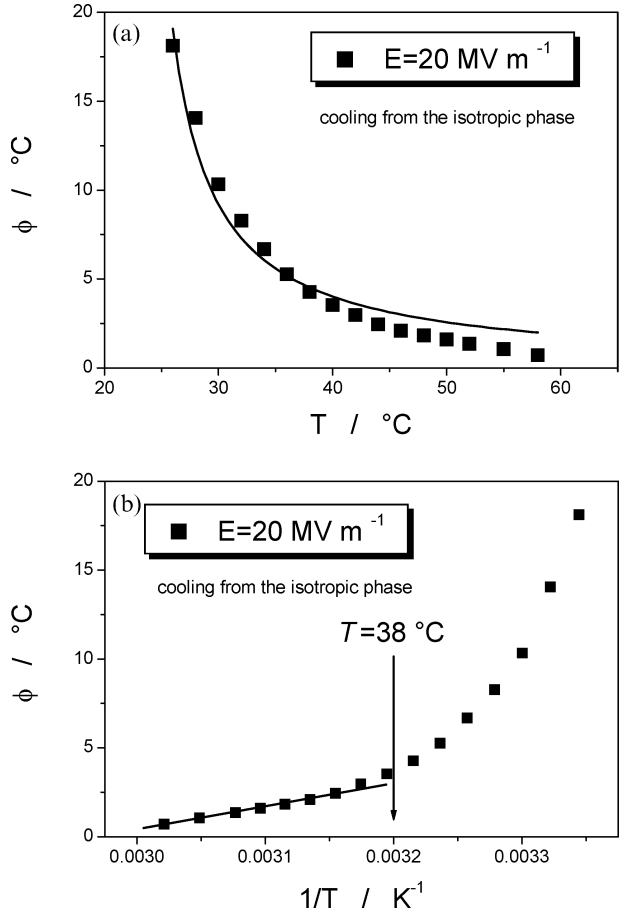

Figure 4. (a) Temperature dependence of the electroclinically induced tilt angle ϕ. The solid line represents the best fit according to Equation (1), demonstrating obvious deviations from pure electroclinic behaviour when applied over the whole SmA* temperature region. (b) Induced tilt angle as a function of reciprocal temperature. Only at temperatures above $T=38^{\circ}C$ is the relation of Equation (1) valid.

a phase transition temperature T_C. Rewriting Equation (2), taking $T_C \approx 23^{\circ}C$ (estimated from the electro-optical response of Figure 4 a) and using a commonly observed value of α ($4 \times 10^4 \, J \, m^{-3} \, K^{-1}$) (*28*), we can estimate the temperature dependence of the effective viscosity, γ. The corresponding behaviour is depicted in Figure 6, again for cooling from the isotropic melt (squares), as well as for heating after tempering the sample for 24 h at $T=25^{\circ}C$ (triangles). Note the increase in viscosity during the tempering process and the observation of identical values on subsequent heating in the temperature region above $T=38^{\circ}C$. The estimated values in this region are approximately one order of magnitude larger as compared to the soft-mode viscosities obtained for commercial low molar mass materials (*29*), which is in accordance with the bulky nature and the larger molar mass of the here investigated material.

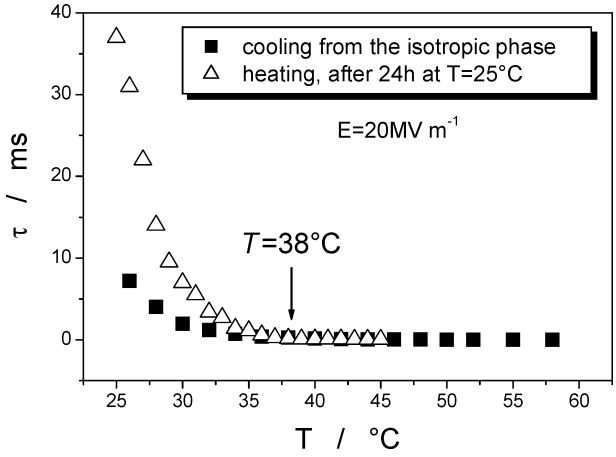

Figure 5. Temperature dependence of the response time τ for cooling from the isotropic phase (squares) and subsequent heating after tempering the sample for 24 h at $T=25^{\circ}C$ (triangles). The response time is found to increase due to tempering, but by heating above a temperature of approximately 38°C it resumes the same temperature dependence as previously observed on cooling.

In the context of the glass transition, the temperature dependence of the viscosity is often discussed in terms of the Vogel–Fulcher–Tamman (VFT) equation: $\log \gamma = A + \mathbf{B}/(T - C)$ or $\gamma(T) = \gamma_0 \exp(DT_0/(T - T_0))$, where T_0 is called the Vogel temperature. It should be noted that the VFT equation describes the shear viscosity, in contrast to the rotational or soft-mode viscosity as discussed in this study. In addition, the VFT description can not be applied to the present system exhibiting two distinct temperatures, T_C and T_0, as the mathematical

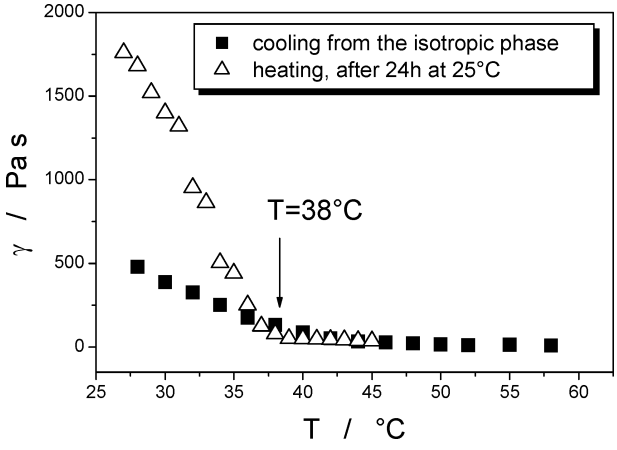

Figure 6. Temperature dependence of the effective viscosity γ for cooling from the isotropic phase (squares) and subsequent heating after tempering the sample for 24 h at $T=25^{\circ}C$ (triangles). The viscosity is found to increase due to tempering, but by heating above a temperature of approximately 38°C it resumes the same values as previously observed on cooling.

form of the equation implies a single divergence temperature T_0. We thus resort to a very similar, general description of the temperature dependence of the viscosity following an Arrhenius behaviour:

$$\gamma = \gamma_0 \exp\left(-\frac{E_a}{k_B T}\right), \tag{3}$$

where E_a is the activation energy and k_B the Boltzmann constant (*30*). From the temperature dependence of the effective viscosity, we can estimate the activation energy for the switching process by an Arrhenius plot, which is shown in Figure 7 (a) for the cooling (squares) and in Figure 7 (b) for the heating process after 24 h tempering (triangles). Pronouncedly observed for the heating process (Figure 7 (b)), but also indicated during cooling from the isotropic melt (Figure 7 (a)), three temperature regimes of differing activation energy can clearly be detected. In both the cooling as well as the heating process, the activation energies in the high-temperature regime are somewhat smaller than those obtained in the low-temperature regime: 101 kJ mol^{-1} compared to 114 kJ mol^{-1} for cooling and 45 kJ mol^{-1} compared to 57 kJ mol^{-1} for heating, respectively. Whereas the high- and the low-temperature regimes exhibit activation energies of at least comparable values, they are separated by a transition temperature range of much higher activation energy; 185 kJ mol^{-1} for cooling and 383 kJ mol^{-1} for heating after tempering. This transition range is centred around the previously encountered temperature of approximately $T \approx 38^\circ$C (40°C on cooling and 36°C on heating after tempering), providing further evidence for a transition within the SmA* phase. It is interesting to note that for the high- and the low-temperature region the activation energies determined after tempering are approximately a factor of two smaller than those obtained for cooling from the isotropic phase, whereas the activation energy in the transition region is about a factor of two larger.

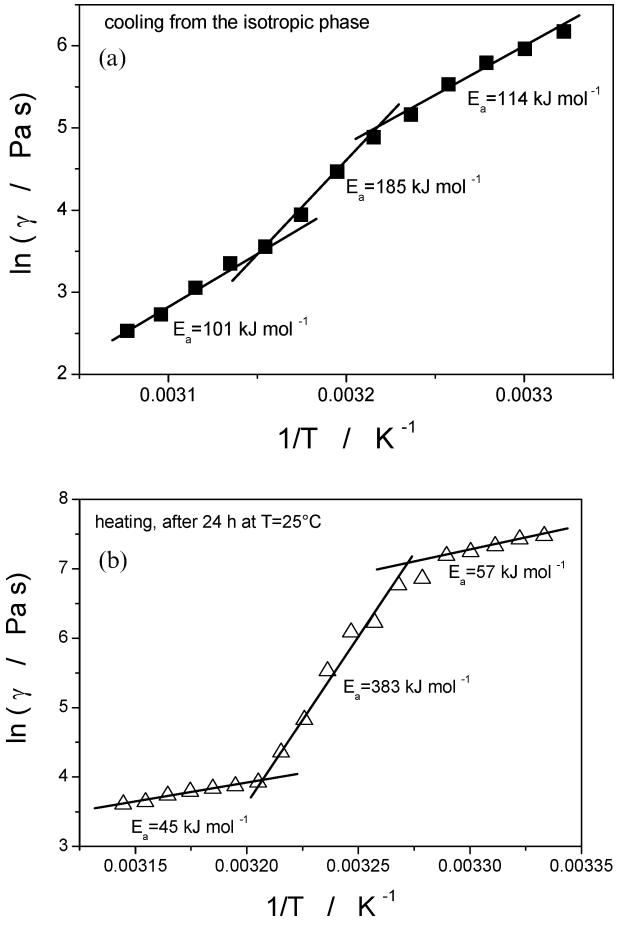

Figure 7. Arrhenius plot of the viscosity for (a) cooling from the isotropic phase (squares) and (b) for heating after tempering the sample for 24 h at $T=25^\circ$C (triangles). A determination of the respective activation energies, E_a, indicates a transition region around 38°C. For a more detailed discussion see the text.

Considering the unusual behaviour of the investigated material, it is worthwhile to study the time dependence of the physical parameters, covering a period of at least two days at isothermal conditions. Cooling the sample to a temperature of $T=45^\circ$C (well above the transition at $T \approx 38^\circ$C and well below the I–SmA* two-phase region), the induced tilt angle ϕ, as well as the electro-optical response time, τ, and thus also the estimated effective viscosity, γ, were constant with time over several days. This clearly indicates a thermodynamically stable SmA* phase at this temperature. Figure 8 depicts the more interesting case of the corresponding time behaviour at $T=25^\circ$C, well below the transition at approximately $T \approx 38^\circ$C, investigated over a time period of more than two days. For this investigation the sample was slowly cooled across the I–SmA* transition to obtain good alignment and was subsequently cooled rather quickly from the SmA* phase at elevated temperatures down to $T=25^\circ$C. It should be stressed that no texture changes whatsoever were observed during the latter cooling process. After isothermal conditions were reached at $T=25^\circ$C, a constant induced tilt angle, ϕ (Figure 8 (a)), response time, τ (Figure 8 (b)), and effective viscosity, γ (Figure 8 (c)), were observed over a time period of approximately five hours. Only after this time were significant changes in the determined properties observed (Figure 8, note the logarithmic time scale). The induced tilt angle decreased towards zero over a period of approximately two days, accompanied by a large increase in response time and viscosity.

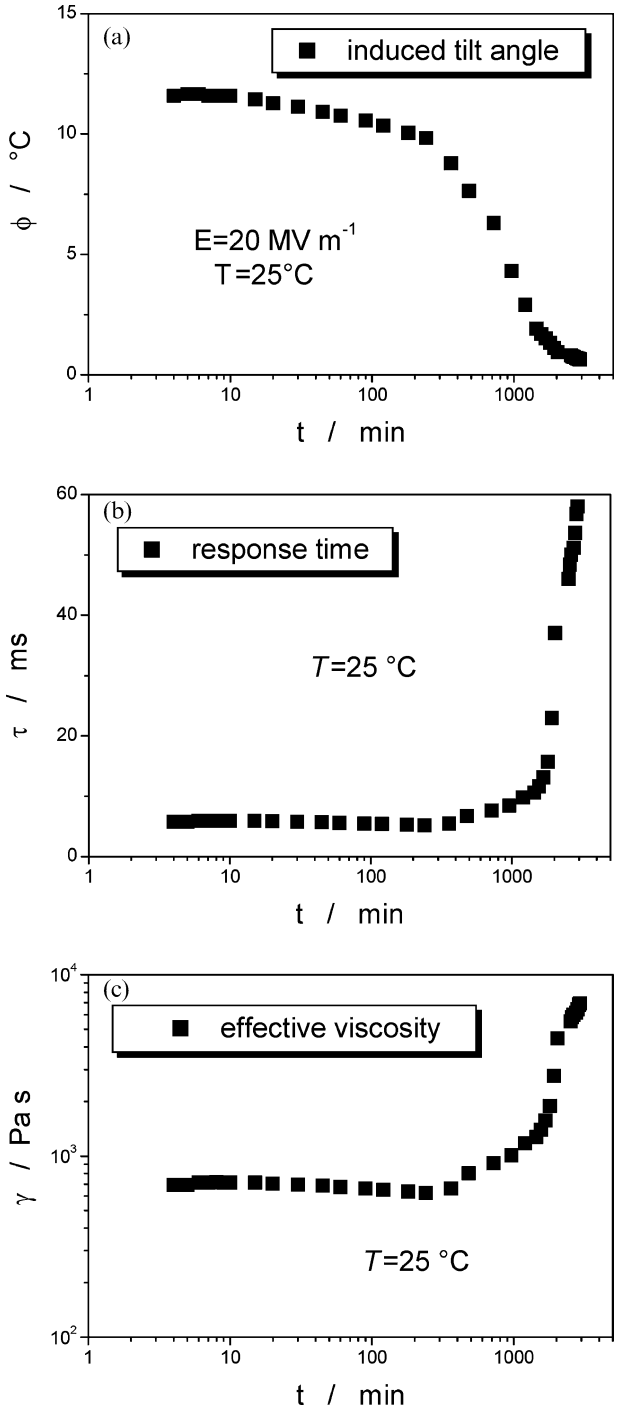

Figure 8. Time dependence of (a) the induced tilt angle ϕ, (b) the response time τ and (c) the effective viscosity γ at isothermal conditions of $T=25^{\circ}C$, below the transition within the SmA* phase. Values of all parameters are practically constant for several hours, before a diminishing electro-optical response is observed, accompanied by diverging response times and viscosity. Note the logarithmic time scale, which covers a period of more than two days.

Taking all of the presented experimental data into account, we propose the following phase behaviour of the compound under investigation: lowering the temperature from the isotropic liquid, a common SmA* phase is formed, which exhibits a relatively large electroclinic response, diverging as room temperature is approached. On cooling as well as heating, the sample exhibits a transition at a temperature of approximately $T=38^{\circ}C$, which can not be related to a transition into any phase other than between SmA* phases. No *qualitative* changes of the texture appearance or the electro-optical behaviour could be observed, although *quantitative* changes of physical parameters and deviations from the general electroclinic behaviour were clearly detected for temperatures below 38°C. The observed behaviour at 38°C may be attributed to a transition from a smectic layer structure with freely flexible molecular groups to one where the phenyl-containing side-groups become hindered, e.g. by changing from a non-intercalated to an intercalated structure on cooling (or vice versa on heating). Such transitions have for example been reported for lipid bilayers (*31*). There is an increase in the viscosity, while retaining enough flexibility for the mesogenic core, which is largely responsible for the electro-optical response, to reorient and respond to electric field application. Further cooling towards room temperature then results in the material undergoing a second transition into a glassy state, where the molecular motion of the bulky cholesteryl group slowly ceases, as does the electro-optical response. After several days at low temperatures the material then exhibits the properties of a true orientationally ordered glass.

Considering the large induced tilt at room temperature of approximately $\pm 20^{\circ}$, it is worthwhile to point out the applicational aspects of such a material. These are based on the fact that the direction of the optical axis can be selected by application of a suitable dc electric field when heating the material above 38°C. Subsequent cooling to room temperature will then freeze this direction into a glassy state. This can be of importance for long-term stable, completely non-mechanical, but still variable optical devices, optical data storage or variable second harmonic generation (SHG) devices.

4. Conclusions

Employing differential scanning calorimetry, polarising optical microscopy, electro-optical and electric measurements, we have characterised a low molar mass cholesteryl-carbonate with a peculiar behaviour of its physical parameters at low temperatures. Evidence is presented that the material exhibits a

transition within the SmA* phase, while retaining all of the qualitative features of the phase. No texture change is observed, and the electric and electro-optical response stays purely electroclinic. Only the response time and the rotational viscosity exhibit a deviation from the classic electroclinic behaviour at lower temperatures. This may be attributed to a partial hindrance of the flexible side group attached to the cholesteryl-based mesogenic core, possibly through a transition from a non-intercalated to an intercalated structure on cooling. At lower temperatures the material undergoes a further transition into a glassy state.

Given the very large induced tilt angles of up to $\pm 20^{\circ}$, together with the possibility of freezing an electrically selectable non-centrosymmetric, polar structure into a glass is intriguing for application devices, including second harmonic generation. The ability to change the selected polar properties in orientation as well as in magnitude, by heating above the transition within the SmA* phase and subsequent cooling into the glassy state provides an additional flexibility for device construction, which is absent from common solid state materials.

Acknowledgements

I would sincerely like to thank V. Vill (University of Hamburg, Germany) for providing the investigated compound and V. Görtz (University of York, UK) for the DSC measurements.

References

(1) Reinitzer F. *Monatsh. Chem.* **1888**, *9*, 421–441.
(2) Lehmann O. *Z. Phys. Chem.* **1889**, *4*, 462–467.
(3) Vorländer D.; Selke W. *Z. Phys. Chem.* **1928**, *129*, 435.
(4) Vill V.; Thiem J.; Rollin P. *Z. Naturforsch.* **1990**, *45a*, 1205–1210.
(5) Doremus R.H. *Glass Science*, 2nd ed.; John Wiley & Sons: New York, 1994.
(6) Donth E.-J. *The Glass Transition: Relaxation Dynamics in Liquids and Disordered Media*; Springer: Berlin, 2001.
(7) Angell C.A., Egami T., Kieffer J., Nienhaus U., Ngai K.L. (Eds), *Structure and Dynamics of Glasses and Glass Formers*, Materials Research Society: Warrendale, PA, 1997.
(8) Debenedetti P.G.; Stillinger F.H. *Nature* **2001**, *410*, 259–267.
(9) Angell C.A.; Ngai K.L.; McKenna G.B.; McMillan P.F.; Martin S.W. *J. Appl. Phys.* **2000**, *88*, 3113–3157.
(10) Cowie J.M.G. *Polymers: Chemistry & Physics of Modern Materials*, 2nd ed.; Blackie Academic & Professional: London, 1996.
(11) Elias H.-G. *An Introduction to Polymer Science*; VCH: Weinheim, 1997.
(12) Greer A.L. *Science* **1995**, *267*, 1947–1953.
(13) Kovalenko N.P.; Krasny Y.P.; Krey U. *Physics of Amorphous Metals*; Wiley-VCH: Berlin, 2001.
(14) Garoff S.; Meyer R.B. *Phys. Rev. Lett.* **1977**, *38*, 848–851.
(15) Clark N.A.; Lagerwall S.T. *Appl. Phys. Lett.* **1980**, *36*, 899–901.
(16) Elschner R.; Macdonald R.; Eichler H.J.; Hess S.; Sonnet A.M. *Phys. Rev. E* **1999**, *60*, 1792–1798.
(17) Tsuji K.; Sorai M.; Seki S. *Bull. Chem. Soc. Japan* **1971**, *44*, 1452.
(18) Lydon J.E.; Kessler J.O. *J. Phys.* **1975**, *36*, C1-153–C1-157.
(19) Wedler W.; Demus D.; Zaschke H.; Mohr K.; Schäfer W.; Weissflog W. *J. Mater. Chem.* **1991**, *1*, 347–356.
(20) Dehne H.; Roger A.; Demus D.; Diele S.; Kresse H.; Pelzl G.; Wedler W.; Weissflog W. *Liq. Cryst.* **1989**, *6*, 47–62.
(21) Schäfer W.; Uhlig G.; Zaschke H.; Demus D.; Diele S.; Kresse H.; Ernst S.; Wedler W. *Mol. Cryst. Liq. Cryst.* **1990**, *191*, 269–276.
(22) Attard G.S.; Imrie C.T.; Karasz F.E. *Chem. Mater.* **1992**, *4*, 1246–1253.
(23) Eichler H.J.; Heppke G.; Macdonald R.; Schmid H. *Mol. Cryst. Liq. Cryst.* **1992**, *223*, 159–168.
(24) Attard G.S.; Imrie C.T. *Liq. Cryst.* **1992**, *11*, 785–789.
(25) Rudquist P., Ph.D. Thesis, Chalmers University of Technology, 1997.
(26) Miyasato K.; Abe S.; Takezoe H.; Fukuda A.; Kuze E. *Jap. J. Appl. Phys. Lett.* **1983**, *22*, L661–L663.
(27) Lagerwall S.T. *Ferroelectric and Antiferroelectric Liquid Crystals*; Wiley-VCH: Weinheim, 1999.
(28) Giesselmann F.; Zugenmaier P. *Phys. Rev. E* **1995**, *52*, 1762–1772.
(29) Buivydas M., Ph.D. Thesis, Chalmers University of Technology, 1997, reproduced by Lagerwall (*27*), chapter 7.2.
(30) Kneppe H.; Schneider F. *Mol. Cryst. Liq. Cryst.* **1981**, *65*, 23–37.
(31) Kind R.; Blinc R.; Arend H.; Muralt P.; Slak J.; Chapuis G.; Schenk J.; Zeks B. *Phys. Rev. A* **1982**, *26*, 1816–1819.